

# Real-Time Monitoring of Cancer Cell Metabolism and Effects of an Anticancer Agent using 2D In-Cell NMR Spectroscopy\*\*

He Wen, Yong Jin An, Wen Jun Xu, Keon Wook Kang, and Sunghyoun Park\*

**Abstract:** Altered metabolism is a critical part of cancer cell properties, but real-time monitoring of metabolomic profiles has been hampered by the lack of a facile method. Here, we propose real-time metabolomic monitoring of live cancer cells using  $^{13}\text{C}_6$ -glucose and heteronuclear two-dimensional (2D) NMR. The method allowed for metabolomic differentiation between cancer and normal cells on the basis of time-dependent changes in metabolite concentrations. Cancer cells were found to have large in- and out-flux of pyruvate as well as increased net production of alanine and acetate. The method also enabled evaluation of the metabolic effects of galloflavin whose anticancer effects have been attributed to its specific inhibition of lactate dehydrogenase. Our approach revealed previously unknown functional targets of galloflavin, which were further confirmed at the protein levels. Our method is readily applicable to the study of metabolic alterations in other cellular disease model systems.

It is now increasingly accepted that altered metabolism is a critical feature of cancer cells.<sup>[1]</sup> For example, new metabolic roles of p53, a tumor suppressor, and MYC, an oncogenic protein, have been discovered.<sup>[2]</sup> Still, many of the metabolic studies on cancer have focused on the roles of proteins, and the characterization of mutations or expression levels has been at the heart of the experimental investigations. More recently, the relevance of small molecular metabolites in cancer metabolism began to draw attention. As important examples, 2-hydroxyglutarate, fumarate, and succinate have been designated as “oncometabolites” due to their active roles in tumorigenesis.<sup>[3]</sup>

This research on small molecular metabolites has been driven mostly by metabolomics which assesses the levels of many metabolites in a system. Still, a majority of cellular metabolomic research has remained concerned with measuring the steady-state concentrations of metabolites rather than their actual changes. Experimentally, metabolites are extracted from the system, which necessarily involves the destruction of the experimental system such as cells. These approaches make the measurement of real-time metabolic flux, the true indication of metabolic activity, impossible; thus, metabolic flux has been estimated indirectly through the analysis of complicated isotopic incorporation patterns or mathematical modeling.<sup>[4]</sup> Although  $^{13}\text{C}$ -hyperpolarized metabolites can give real-time metabolic flux information, their short lifetime ( $\approx 1$  min) and extreme technical requirements have limited their general use, except for very specialized cases.<sup>[5]</sup>

The term “in-cell NMR” has been used for studies observing mostly biological macromolecules in live cells<sup>[6]</sup> or given metabolites of interest in *E. coli* or yeasts.<sup>[7]</sup> On the other hand, mammalian metabolites have long been studied “in-cell” using  $^{13}\text{C}$  NMR spectroscopy with perfused cells in a spectrometer.<sup>[8]</sup> These studies have provided important insights into long-term kinetic and metabolic flux information. Still, they featured complicated apparatuses, uncommon/custom NMR hardware, and inherently low sensitivity, which may have hampered wider usage by general NMR and metabolism researchers. Therefore, a simpler and more sensitive approach for the real-time profiling of metabolic flux in mammalian cells has been desired. Here, we used  $^1\text{H}$ -detected 2D-heteronuclear single quantum coherence (HSQC) spectra for fast, simple, sensitive, and high-resolution monitoring of metabolites from cells in standard NMR tubes (2D HSQC in-cell NMR metabolomics). The method was applied to cancer (HepG2) and normal (NKNT-3) cell metabolism and the mechanism of an anticancer agent without any a priori assumption.

The method starts with the harvesting of cells grown in normal cell culture media (with 10% serum) and their resuspension in an NMR medium (glucose-free medium with 10% dialyzed serum) supplemented with  $^{13}\text{C}_6$ -labeled glucose. The cells ( $5 \times 10^7$ ) were spun in an NMR tube with a weak centrifugal force (30 g for 100 s) to allow sedimentation, enough to cover the active coil region. This step addresses the cell precipitation and the changes in magnetic susceptibility.<sup>[9]</sup> Then, the NMR tube was put into a spectrometer, and a series of HSQC spectra (total 26; ca. 5 min each) were obtained for the metabolomic study with high sensitivity and confident assignments. The cell viability (by trypan blue) did not change much throughout the experiment with the

[\*] Dr. H. Wen,<sup>[‡]</sup> Y. J. An,<sup>[‡]</sup> W. J. Xu, Prof. S. Park  
College of Pharmacy, Natural Product Research Institute  
Seoul National University  
Sillim-dong, Gwanak-gu, Seoul, 151-742 (Korea)  
E-mail: psh@snu.ac.kr

Prof. K. W. Kang  
Research Institute of Pharmaceutical Sciences  
Seoul National University  
Sillim-dong, Gwanak-gu, Seoul, 151-742 (Korea)

[‡] These authors contributed equally to this work.

[\*\*] This study was supported by grants from the National R&D Program for Cancer Control (1420290) and the Korean Health Technology R&D Project (H113C0015) from the Ministry of Health & Welfare, Republic of Korea and by the Basic Science Research Program through the National Research Foundation of Korea funded by the Ministry of Education, Science, and Technology (2012011362 and 200993144).



Supporting information for this article is available on the WWW under <http://dx.doi.org/10.1002/anie.201410380>.

maximum difference of 6.7% (Figure S1A). Although the medium around the cells turned somewhat yellow, the intracellular pH did not drop much, based on the constant acetate chemical shifts (Figure S1B). It should be noted that the intracellular pH is always higher than the outside pH at  $\text{pH} < 7.4$ .<sup>[10]</sup> In addition, the metabolic status (by adenylate energy charge) was within a normal range for mammalian tissues ( $> 0.75$ )<sup>[11]</sup> with the lowest value of 0.803 (Figure S1C). Furthermore, very different relative levels of peaks from the medium versus entire sample confirmed no nonspecific leakage of metabolites (Figure S1D). These show that the cells in the NMR tubes are live and metabolically relevant.

The HSQC spectrum of HepG2 cells exhibited over 50 peaks in just 5 min of NMR acquisition as well as rare peak overlap, except those for  $^{13}\text{C}_6$ -labeled glucose (input) (Figure 1A). Time-dependent intensity changes were followed for

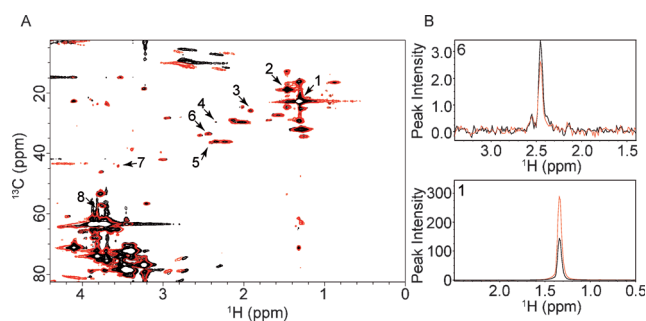


**Figure 1.** Time-dependent changes in HSQC spectra of HepG2 cells over 2 hour and 10 min after the addition of  $^{13}\text{C}_6$ -glucose. A) Only the first (black) and the last (red) spectra are overlaid. (1: lactate, 2: alanine, 3: acetate, 4: pyruvate, 5: succinate, 6:  $\alpha$ -ketoglutarate, 7: glycine, 8: serine; see Table S1 and Figure S2 for the assignments). B) One-dimensional trace for two compounds (1 and 6).

the peaks, and the assignments were obtained for those showing significant changes (Figure 1B; see Figure S2 and Table S1 for the assignments). The data also confirmed that the line widths remained essentially the same throughout the experiments. The identified metabolites suggested that the changes in the key metabolic pathways, such as glycolysis, pyruvate metabolism, and their downstream steps, can be monitored in live cells. Although we did not analyze the time-dependent changes of glutamate, the incorporation of the  $^{13}\text{C}$  label into the C4 of glutamate confirmed the existence of the functional tricarboxylic acid (TCA) cycle in our system (Figure S2D). We also established a procedure to measure the absolute concentration of the metabolites for in-cell NMR metabolomics (see the Supporting Information (SI) Methods section and Figure S3).

The approach was then applied to characterizing cancer-specific metabolomic features in terms of the absolute metabolite concentrations in real-time using cancer (HepG2) and normal (NKNT-3) cells (Figure 2). The cancer cells exhibited much higher production rates for lactate, alanine, and acetate. Intriguingly, these three are the major metabolites synthesized from pyruvate through one biochemical step. Therefore, their higher net production indicates that out-flux of pyruvate is higher in cancer cells than in normal

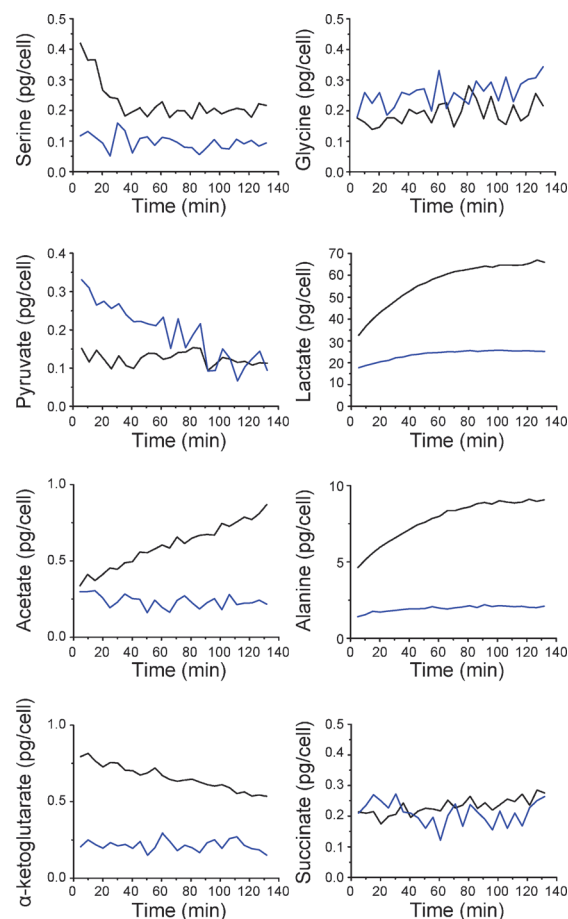


**Figure 2.** Real-time flux comparison in live normal (NKNT-3) and cancer (HepG2) cells. Time-dependent metabolic changes between normal (blue) and cancer (black) cells were obtained using in-cell NMR metabolomics approach. The metabolite quantified in their absolute concentrations (picogram per cell).

ones. Pyruvate, the final product of glycolysis, was unique in exhibiting net higher consumption in normal cells (out-flux  $>$  in-flux) while showing a steady level in cancer cells (out-flux  $\approx$  in-flux). Given the larger out-flux of pyruvate from cancer cells, the in-flux of pyruvate in cancer cells should be much larger than that in normal cells. As labeled pyruvate should come from labeled glucose through glycolysis, this observation nicely supports the Warburg effect in cancer cells, the increased glycolytic flux and concomitant higher production of lactate.<sup>[12]</sup> Consistently, we also observed higher lactate production in cancer cells when  $^{13}\text{C}_3$ -pyruvate was used (Figure S4).

Our results also revealed previously little-noticed metabolic alterations in cancer cells: the increase in the net production of alanine and acetate,<sup>[13]</sup> which may also be cancer-specific metabolic features that can serve as new targets for therapeutic intervention. In fact, alanine aminotransferase, an enzyme synthesizing alanine from pyruvate, was shown to be important in maintaining a cancer-specific growth phenotype of colon cancer cells.<sup>[14]</sup>

The levels of glycine and succinate were similar and constant in both cell types. In comparison, the consumption

rate of  $\alpha$ -ketoglutarate ( $\alpha$ -KG) was slightly higher in cancer cells, which may be due to  $\alpha$ -KG's role as an intermediate for multiple reactions, such as transamination and dioxygenation.<sup>[15]</sup> For glycine and serine, their one carbon metabolism is increasingly recognized for the nucleotide synthesis in cancer.<sup>[16]</sup> However, direct glycine metabolism by glycine dehydrogenase seems dispensable in, or even inhibitory for, cancer proliferation.<sup>[17]</sup> Therefore, the similar glycine metabolism in cancer and normal cells suggests that glycine for the higher nucleotide synthesis in cancer cells may be supplied from the available serine/glycine pool rather than synthesized from glucose. The general trends of the metabolic flux difference between normal and cancer cells were maintained throughout the experiment. Still, some changes, that is, for serine, are noted at a later stage, possibly due to the cell's different responses to hypoxia. These may need to be considered in comparing the results with those from perfused cells without hypoxia.<sup>[8]</sup>

We next applied the approach to an investigation of the effects of an anticancer agent, galloflavin, a recently identified lactate dehydrogenase (LDH)-specific inhibitor,<sup>[18]</sup> especially in the metabolic perspective. We followed the changes in the metabolic flux after the galloflavin treatment in HepG2 cells (Figure 3). The overall pattern of the metabolic shifts was strikingly similar to that between cancer and normal cells, as evident for lactate, alanine, and succinate. These results show that galloflavin not only inhibits pyruvate-to-lactate conversion, but also affects many other metabolic pathways, and that galloflavin's anticancer effects seem to be due to these multifaceted effects rather than to specific inhibition of LDH. This highlights the utility of in-cell NMR metabolomics in addressing the possible mechanism of an anticancer agent.

Interestingly, lactate production was lower in the galloflavin-treated cells until about 110 min, but then, abruptly increased close to the level in the control cells (arrows in Figure 3). This seems to be due to the recovery of the LDH activity through metabolic inactivation of galloflavin. Similar changes were also observed for acetate and alanine, albeit a bit weaker for alanine, but not for  $\alpha$ -ketoglutarate or succinate. Therefore, lactate production seems intimately coupled to the alanine and acetate metabolism, but not immediately to the further downstream metabolism. Overall, our approach provides information on real-time metabolic flux changes by drug molecules, the pharmacokinetic activity profile, and the coupling between metabolic pathways.

The metabolic effects of galloflavin other than the inhibition of LDH were also confirmed for enzymes associated with the measured metabolites (Figure 4). In contrast to LDH, the level of ALT1 was greatly reduced by galloflavin. This shows that galloflavin affects lactate and alanine levels differentially through enzyme activity (LDH) and expression (ALT1). We also observed that pyruvate dehydrogenase (PDH), involved in pyruvate to acetyl-CoA conversion, was not affected, but that the level of phospho-PDH (p-PDH), an inactive form of PDH, was greatly reduced. This is consistent with the increase in the consumption (time-dependent decrease) of pyruvate observed in the galloflavin-treated cells (Figure 3). It also suggests that pyruvate dehydrogenase kinase (PDK), which phosphorylates PDH, may have been

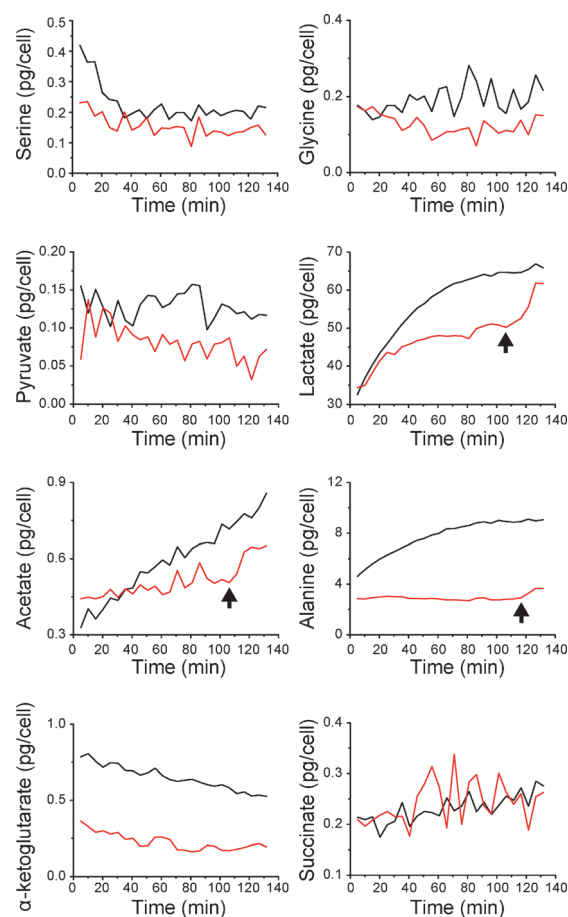


**Figure 3.** Real-time monitoring of the metabolic alteration by galloflavin treatment (5 mM) in HepG2 cells (red). Black is the control HepG2 cells as in Figure 2. The arrows in the graphs indicate the time at which metabolic change occurred for the specified metabolites.

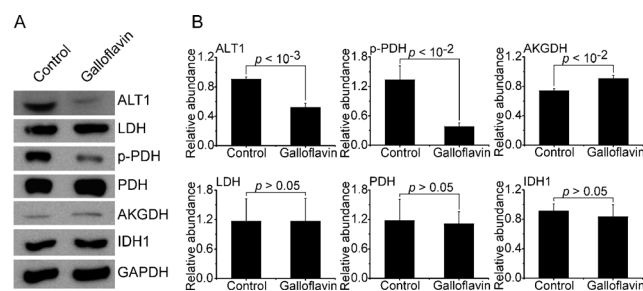


**Figure 4.** Expression levels of enzymes related to the measured metabolites. A) Western blots of alanine aminotransferase 1 (ALT1), lactate dehydrogenase (LDH), pyruvate dehydrogenase and its phosphorylated form (PDH and p-PDH, respectively),  $\alpha$ -ketoglutarate dehydrogenase (AKGDH), and isocitrate dehydrogenase 1 (IDH1) from non-treated (control) and galloflavin-treated (5 mM) HepG2 cells. Glyceraldehyde 3-phosphate dehydrogenase (GAPDH) was used as a loading control. The bar charts represent the comparison of the mean band intensities for the levels of the proteins normalized to that of the GAPDH. A statistical analysis was performed using the Student's *t*-test, and the resulting *p*-values are indicated. The error bars represent the standard deviation (B).

inhibited by galloflavin. The level of  $\alpha$ -ketoglutarate dehydrogenase (AKGDH) was also affected, but to a lesser degree. In comparison, isocitrate dehydrogenase 1 (IDH1) was not greatly affected. Galloflavin has been reported as a selective LDH inhibitor<sup>[18a]</sup> and its activity against cancer cells has been interpreted with respect to its LDH inhibitory activity.<sup>[18b]</sup> However, our in-cell NMR metabolomics driven approach revealed that PDK and ALT1 could be its new targets, and that galloflavin should also be classified as a “functional inhibitor” of PDK and ALT1 and a “functional activator” of PDH.

In conclusion, our approach enabled detailed metabolomic comparison of cancer and normal cells and the identification of new targets of an anticancer agent. It can be straightforwardly extended to the study of other disease-related cell systems.

**Keywords:** cancer · galloflavin · metabolomics · NMR spectroscopy

**How to cite:** *Angew. Chem. Int. Ed.* **2015**, *54*, 5374–5377  
*Angew. Chem.* **2015**, *127*, 5464–5467

- 
- [1] P. S. Ward, C. B. Thompson, *Cancer Cell* **2012**, *21*, 297–308.  
[2] a) A. Terunuma, et al., *J. Clin. Invest.* **2014**, *124*, 398–412; b) P. Jiang, W. Du, X. Wang, A. Mancuso, X. Gao, M. Wu, X. Yang, *Nat. Cell Biol.* **2011**, *13*, 310–316.  
[3] M. Yang, T. Soga, P. J. Pollard, *J. Clin. Invest.* **2013**, *123*, 3652–3658.  
[4] J. K. Sims, S. Manteiga, K. Lee, *Curr. Opin. Biotechnol.* **2013**, *24*, 933–939.  
[5] M. M. Chaumeil, P. E. Larson, H. A. Yoshihara, O. M. Danforth, D. B. Vigneron, S. J. Nelson, R. O. Pieper, J. J. Phillips, S. M. Ronen, *Nat. Commun.* **2013**, *4*, 2429.  
[6] a) D. I. Freedberg, P. Selenko, *Annu. Rev. Biophys.* **2014**, *43*, 171–192; b) R. Hänsel, L. M. Luh, I. Corbeski, L. Trantirek, V. Dotsch, *Angew. Chem. Int. Ed.* **2014**, *53*, 10300–10314; *Angew. Chem.* **2014**, *126*, 10466–10480.  
[7] a) J. Ma, S. McLeod, K. MacCormack, S. Sriram, N. Gao, A. L. Breeze, J. Hu, *Angew. Chem. Int. Ed.* **2014**, *53*, 2130–2133; *Angew. Chem.* **2014**, *126*, 2162–2165; b) S. Y. Rhieu, A. A. Urbas, D. W. Bearden, J. P. Marino, K. A. Lippa, V. Reipa, *Angew. Chem. Int. Ed.* **2014**, *53*, 447–450; *Angew. Chem.* **2014**, *126*, 457–460.  
[8] a) M. P. Gamcsik, K. K. Millis, O. M. Colvin, *Cancer Res.* **1995**, *55*, 2012–2016; b) A. Mancuso, S. T. Sharfstein, S. N. Tucker, D. S. Clark, H. W. Blanch, *Biotechnol. Bioeng.* **1994**, *44*, 563–585; c) J. S. Cohen, R. C. Lyon, *Ann. N. Y. Acad. Sci.* **1987**, *508*, 216–228; d) A. Mancuso, N. J. Beardsley, S. Wehrli, S. Pickup, F. M. Matschinsky, J. D. Glickson, *Biotechnol. Bioeng.* **2004**, *87*, 835–848; e) R. E. Jeffries, J. M. Macdonald, *NMR Biomed.* **2012**, *25*, 427–442.  
[9] B. Bekei, H. M. Rose, M. Herzig, H. Stephanowitz, E. Krause, P. Selenko, *Methods Mol. Biol.* **2012**, *895*, 67–83.  
[10] C. W. Song, R. Griffin, H. J. Park in *Cancer Drug Resistance*, Springer, Berlin, **2006**, pp. 21–42.  
[11] A. G. Chapman, L. Fall, D. E. Atkinson, *J. Bacteriol.* **1971**, *108*, 1072–1086.  
[12] O. Warburg, K. Posener, E. Negelein, *Biochem. Z.* **1924**, *152*, 319–344.  
[13] D. A. Scott, A. D. Richardson, F. V. Filipp, C. A. Knutzen, G. G. Chiang, Z. A. Ronai, A. L. Osterman, J. W. Smith, *J. Biol. Chem.* **2011**, *286*, 42626–42634.  
[14] F. Weinberg, et al., *Proc. Natl. Acad. Sci. USA* **2010**, *107*, 8788–8793.  
[15] a) W. G. Kaelin, Jr., *Cold Spring Harb. Symp. Quant. Biol.* **2011**, *76*, 335–345; b) M. Tönjes, et al., *Nat. Med.* **2013**, *19*, 901–908.  
[16] M. Jain, et al., *Science* **2012**, *336*, 1040–1044.  
[17] C. F. Labuschagne, N. J. van den Broek, G. M. Mackay, K. H. Voudsen, O. D. Maddocks, *Cell Rep.* **2014**, *7*, 1248–1258.  
[18] a) M. Manerba, M. Vettraino, L. Fiume, G. Di Stefano, A. Sartini, E. Giacomini, R. Buonfiglio, M. Roberti, M. Recanatini, *ChemMedChem* **2012**, *7*, 311–317; b) F. Farabegoli, M. Vettraino, M. Manerba, L. Fiume, M. Roberti, G. Di Stefano, *Eur. J. Pharm. Sci.* **2012**, *47*, 729–738.
- 

Received: October 23, 2014

Revised: January 2, 2015

Published online: March 5, 2015